Journal of Chemical Crystallography
https://doi.org/10.1007/s10870-024-01028-z

ORIGINAL PAPER

The Versatility of the Dicyanamide Anion (Dca) as a Bridging Ligand: Synthesis, Structure and Theory of a Unique Ladder Chain Consisting of 2 $\mu_{1,5}$-dca Bridged Dinuclear $Cu_2(dca)_2$ Units with Additional $\mu_{1,3}$-dca Bridges Along the Chain

Yaakoub Saadallah[1] · Zouaoui Setifi[1,2] · Hela Ferjani[3] · Christopher Glidewell[4] · Christian Jelsch[5] · Fatima Setifi[1] · Diego M. Gil[6] · Jorge Echeverria[7] · Jan Reedijk[8]

Received: 22 June 2024 / Accepted: 13 August 2024

Abstract

The synthesis and structural details of a mixed-ligand Cu(II) coordination compound, specifically *catena*-poly[bis(dicyanamido)(1,10-phenanthroline-5,6-dione)copper(II)] **1**, are reported. The title compound was synthesized utilizing a solvothermal method by employing dicyanamide, 1,10-phenanthroline-5,6-dione (phendione) and copper(II) sulfate pentahydrate ($CuSO_4$•$5H_2O$) as the starting materials. The title compound was characterized by standard analytical and spectroscopic methods. The 3D structure was determined by single-crystal X-ray diffraction. Examination of the supramolecular interaction patterns indicates that the stability of the ladder structure is achieved by the bridging dca anions and the presence of weak hydrogen-bonding contacts, specifically C-H···O and C-H···N bonds, as well as C-O/N···π interactions. These interactions together contribute to the formation of a ladder-type infinite chain structure. The generated structure has been theoretically investigated with Hirshfeld surface analysis, QTAIM and NCI analysis to reveal the interaction energies and bonds present inside and between molecules. The non-covalent interactions present in the crystal structure were further investigated theoretically, with particular attention to the cooperative C≡N···π(py) and N···π(hole) interactions involving the dicyanamide ligand and nitrile moieties in the compound. The solid-state stability of compound **1** appears to be strongly influenced by the cooperative effect of H-bonding interactions as well as the C≡N···π(py) and N···π(hole) contacts, as confirmed by theoretical calculations.

Graphical Abstract

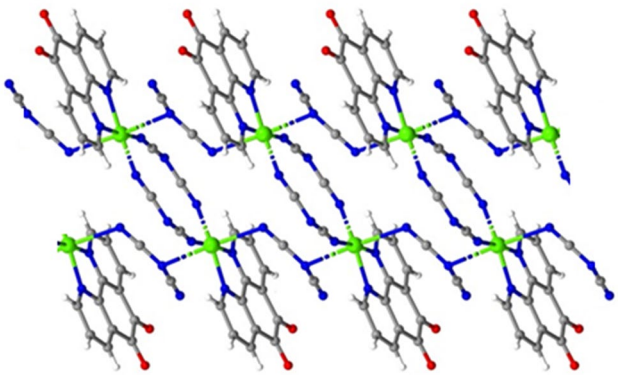

Synthesis, Structure and Theoretical Calculations of a Unique Ladder Chain Containing the Dicyanamido Ligand (dca), Consisting of 2 $\mu_{1,5}$-dca Bridged Dinuclear $Cu_2(dca)_2$Units and Having $\mu_{1,3}$-dca Bridges along the Chain.

One sentence essence:

catena-poly[bis(dicyanamido)(1,10-phenanthroline-5,6-dione)copper(II)] is a unique ribbon ladder, infinite chain structure with two differently bridged dicyanamide anions

Extended author information available on the last page of the article

Published online: 09 September 2024

Keywords Phendione · Dicyanamide · Supramolecular assembly · Hirshfeld surface analysis · Cooperative C≡N···π(py) Stacking; DFT Calculations

Introduction

Coordination polymers containing pseudohalide ligands (like cyanide, azide or thiocyanate anions) have been widely studied for their interesting magnetic and structural properties [1–6]. A more recently introduced pseudohalide ligand is the dicyanamide, dca, ion (see Fig. 1), which has 3 donor N-atoms available, and therefore can potentially bind in various ways, including bridging between two or more metal ions. When it acts as a bridging ligand the dimensionality can increase from 1D to 2D or 3D. The steric shape of the dca anion allows rather rigid bridging between metal ions; in addition the CN groups of dca may in form anion-pi intermolecular or intramolecular interactions [7, 8].

Early work has shown that in its anionic form dca indeed displays a great variability of coordination modes, both bridging and non bridging [9–12]. When the dca anion is used as a bridging co-ligand in coordination polymers with 4,4'-bipy ligands interesting clathration, magnetic and catalytic properties have been reported [13–20]. The discovery of long-range magnetic ordering in $M(dca)_2$ coordination compounds [21–23] has further boosted the search for new types of dca-containing compounds. Amazingly, compounds containing both the end-on and the end-centre bridging have not yet been observed, despite the large variation used in non-bridging co-ligands.

So by using flat co-ligands we now have investigated possible new polymeric structures, making also use of anion-pi interactions to stabilize new structures. Controlling and manipulating of the metal-ligand coordination bonds along with non-covalent interactions [24–26] was therefore employed. Interactions such as hydrogen bonds, C-H···π, π···π, cation···π, lone pair···π and anion···π interactions [27] are expected to play an important role in the stabilization and for the construction of high-dimensional supramolecular architectures [28–30].

In the present work, we explore new binding modes of dca. The results of our hydrothermal synthesis, detailed description of non-covalent interactions of various types and strengths in the crystal structure of the *catena*-poly[bis(dicyanamido)(1,10-phenanthroline-5,6-dione) copper(II)] compound (**1**) will be presented and discussed, using also theoretical methods. The observation of two different bridging modes of dca in a single compound appears to be as unprecedented.

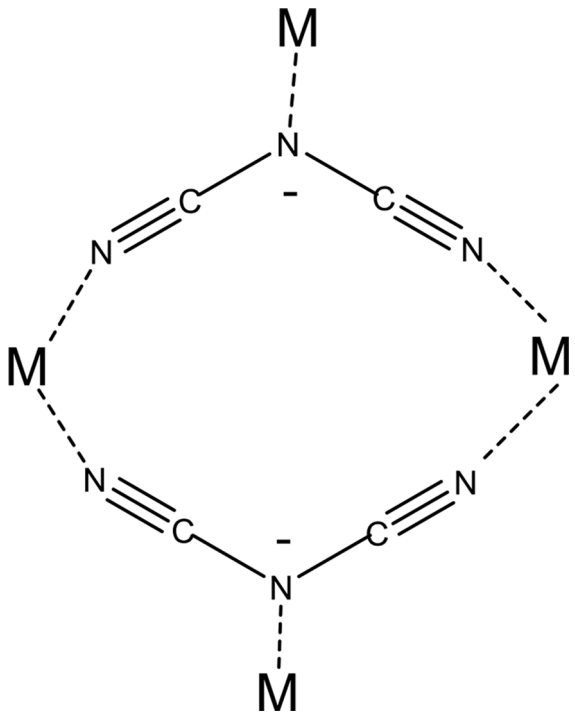

Fig. 1 Potential binding sites for metal ions at the N atoms of the dicyanamide anion, dca

Materials and Methods

Materials

All chemicals were of reagent grade quality, purchased from commercial sources, and used without further purification.

Physical Measurements

Elemental analysis (EA, to analyze %C, H and N) was performed using a PerkinElmer 2400 series II CHNS/O analyzer. The infrared spectrum of the solid compound was recorded at room temperature in the range of 4000–500 cm^{-1} by using a Nicolet 5SX–FTIR spectrometer equipped with a diamond micro-ATR accessory and working with OMNIC software.

Synthesis and Crystallization

All used chemicals were reagent grade, procured from commercial sources, and used without purification. The solvents were purified by standard procedures.

$CuSO_4$•$5H_2O$ (25 mg, 0.1 mmol), 1,10-phenanthroline-5,6-dione (21 mg, 0.1 mmol) and Nadca (18 mg, 0.2 mmol) were dissolved in 20 mL of H_2O/DMF (v/v, 3:1) and then the solution was sealed in a 25 mL Teflon reactor and kept under autogenous pressure at 403 K for 2 days. After cooling to room temperature

at a rate of 10 Kh^{-1}, green crystals of compound **1** were obtained (yield 44%). Anal. Calcd. for $C_{16}H_6CuN_8O_2$: C, 47.35; H, 1.49; N, 27.61%. Found: C, 47.07; H, 1.58; N, 27.75%. Main IR bands (ATR, cm^{-1}): ν(CN): 2302, 2241, 2172 cm^{-1}.

Single-Crystal X-Ray Diffraction

Suitable single crystals of **1** were chosen for an X-ray diffraction study. Data collection was performed on a Rigaku Oxford Diffraction Xcalibur diffractometer with graphite-monochromated Mo Kα radiation ($\lambda = 0.71073$ Å). The structure was solved using the program SHELXT 2014/5 [31] and refined using SHELXL 2014 [32]. Empirical absorption corrections were performed using the CrysAlis PRO program [33]. All non-hydrogen atoms were refined anisotropically. All H atoms were located in difference maps, and then treated as riding atoms in geometrically idealized positions with C-H distances of 0.95 Å and $U_{iso}(H) = 1.2U_{eq}(C)$. A riding model for the H atoms was employed as it is rarely, if ever, fruitful to attempt the refinement of H-atom coordinates using X-ray diffraction data. It is worth noting here that whereas X-ray diffraction provides distances between the centroids of electron density, neutron diffraction would provide distances between the atomic nuclei. For most bonds X-Y, the distances deduced using the two techniques are usually identical within experimental uncertainty. However, for X-H bonds, the centroids of the electron density are invariable closer than the atomic nuclei, consequent upon the absence of non-valence shell (core) electrons in H atoms, and it is thus inappropriate to regard either one of the deduced distances as more 'real' or 'correct' than the other. Details of crystal data, data collection, and structure solution and refinement are summarized in Table 1.

Structure analysis was performed using the Mercury 4.0 program [34]. Crystallographic data is deposited on the CCDC under deposition number 2,296,121. The corresponding CIF file can be accessed free of charge through the access structure applet on the CCDC webpage (https://www.ccdc.cam.ac.uk/structures).

Computational Methods

The energies of the self-assembled dimers of compound **1** were calculated using the crystallographic coordinates at the DFT level using the M062X functional [35] and the def2-TZVP [36] basis set. For all calculations, the Gaussian-16 program [37] was used. The interaction energies were computed with correction for the basis set superposition error (BSSE) employing the Boys-Bernardi counterpoise method [38]. The molecular electrostatic potential (MEP) analysis has been performed at the same level of theory. The quantum theory of atoms in molecules (QTAIM) analysis [39] has been performed by using the Multiwfn program [40] and visualized with the VMD software [41]. The use of NCI plot isosurfaces is a very important tool to evaluate non-covalent interactions because they show the molecular regions involved in interactions [42]. The NCI plot surfaces were computed at the M062X/def2-TZVP level of theory and represented using VMD [41]. The color scheme is red-yellow-green-blue, with red and blue colors for repulsive and attractive interactions, respectively. Finally, the natural bond orbital (NBO) analysis [43] has been performed to unveil possible charge transfer processes in compound 1.

Table 1 Crystallographic data and refinement details for compound **1**

Empirical formula	$C_{16}H_6CuN_8O_2$
Formula weight	405.84
Crystal system, space group	Monoclinic, $P2_1/c$
Temperature	150 K
a, b, c (Å)	7.9596 (3), 30.2311 (11), 6.6615 (3)
β (°)	110.509 (1)
V (Å^3)	1501.34 (10)
Z	4
Radiation type	MoK_α
μ (mm^{-1})	1.49
Crystal size (mm)	0.35 × 0.19 × 0.12
Shape/Color	Block/green
T_{min}/T_{max}	0.735/0.841
No. of measured, independent and observed [$I > 2\sigma(I)$] reflections	63,221, 4595, 4322
R_{int}	0.032
R [$F^2 > 2\sigma(F^2)$]/ $wR(F^2)$/ S	0.031/0.079/1.16
Number of reflections	4595
Number of parameters	244
$\Delta\rho_{max}/\Delta\rho_{min}$ (e Å^{-3})	0.53/-0.39
CCDC number	2,296,121

Results and Discussion

Structure Description

In the structure of *catena*-poly[bis(dicyanamido)(1,10-phenanthroline-5,6-dione)copper(II)], **1**, $[(C_2N_3)_2(C_{12}H_6N_2O_2)Cu]$, the Cu center adopts the usual (4 + 2) coordination (Fig. 2): the four equatorial Cu-N distances are clustered around 2.0 Å, while the axial distances are both in excess of 2.5 Å (Table 2). The intramolecular bond distances and angles are normal and uneventful. The Cu geometry is typical for Cu(II) with 4 short equatorial ligand and 2 semi-coordinating axial Cu-N contacts,

Two differently bridged dca ligands are present. Two of the equatorial sites are occupied by a pair of inversion-related dicyanamido ligands that are coordinated via the terminal N

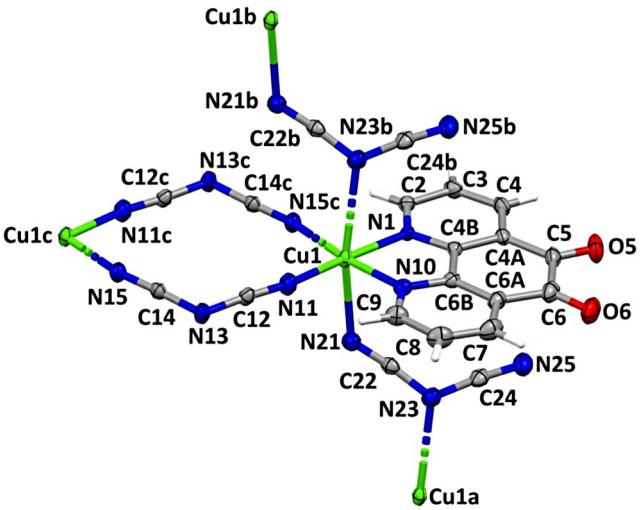

Fig. 2 The structure of the compound shows the different coordination modes of the two dicyanamido ligands (with N13, resp.N23). Displacement ellipsoids are drawn at the 50% probability level and the atoms marked with 'a', 'b' or 'c' are at the symmetry positions (x, y, $-1+z$), (x, y, $1+z$) and (1 - x, 1 - y, 1 - z), respectively

Table 2 Cu-N distances (Å)

Cu-N1	1.9936 (12)	Cu-N10	2.0103 (13)
Cu-N11	1.9545 (15)	Cu-N15^{i}	1.9606 (14)
Cu-N21	2.5094 (13)	Cu-N23^{ii}	2.7359 (14)

Symmetry codes: (i) 1 - x, 1 - y, 1- z ; (ii) x, y, $1+z$

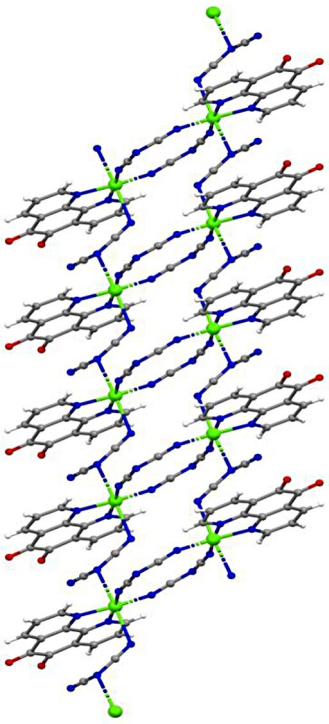

Fig. 3 Part of the crystal structure showing the formation of a coordination polymer ribbon running parallel to [001]

Table 3 Hydrogen-bond geometry (Å, °)

D-H···A	D-H	H···A	D···A	D-H···A
C3-H3···N21^{iii}	0.95	2.54	3.312 (2)	139
C8-H8···O5^{iv}	0.95	2.36	3.102(3)	134

Symmetry codes: (iii) x-1, y, z; (iv) x + 1, -y + 3/2, z + 1/2

atoms, thus generating an 12-membered ring (Fig. 2); such 12-membered rings, as schematically shown in Fig. 1, are known in the literature, and a CSD search (2023) has generated over 20 structures with a variety of metal ions [44]. The other two equatorial sites are occupied by the bidentate 1,10-phenanthroline-5,6-dione, coordinated via the N atoms. By contrast, the second dicyanamido ligand bridges two Cu centers related by translation along [001], in each case via one of the axial sites (Fig. 2), but now both the central N atom and one of the terminal N atoms are involved. The involvement of the central N is quite unusual, although not hitherto unknown [45]; but the two different modes in one single compound are unprecedented to the best of our knowledge.

The resulting coordination polymer takes the form of a ribbon ladder of spiro-fused rings, in which 12-membered rings centered at (0.5, 0.5, 0.5+n) alternate with 20-membered rings centered at (0.5, 0.5, n), where n represents an integer in each case (Fig. 3). Within the ribbon, the shortest Cu···Cu distance along the chain is 6.661(3) Å, while that across the 12-membered ring is 7.063(3) Å. As said above there are two distinct modes of binding for the two independent dicyanamide ligands: one forms double bridges between two metal centers, with each using the two terminal N atoms, while the other employs one terminal N atom and the central amidic N atom to bridge Cu(II) ions. So, compound 1 represents the first example of a phendione 3D polymeric system containing two differently bridging dca ligands between the same paramagnetic metal ions.

There are two short intermolecular contacts involving C-H bonds (Table 3; Fig. 4), but both exhibit C-H···A (A = N or O) angles less than 140°, and therefore cannot be regarded as being structurally significant [46].

There are four short contacts between N or O atoms and adjacent five and six-membered rings (Table 4; Fig. 5). The contact involving a pyridyl ring lies within the coordination polymer ribbon, and so it has no influence on the overall dimensionality of the structure. The other two contacts both involve the quinonoid ring, which is far from aromatic, as evidenced by the long bond C5-C6, 1.548(2) Å, linking the two carbonyl units. The two ribbons are linked by C-O···π stacking interactions involving the five-membered ring enclosing the Cu atom (Table 4; Fig. 5). These weak non-covalent interactions help to stabilize and establish a 2D network.

Contacts on the Hirshfeld Surface

Analysis of intermolecular interactions using the Hirshfeld surface represents a tool to gain detailed insight into

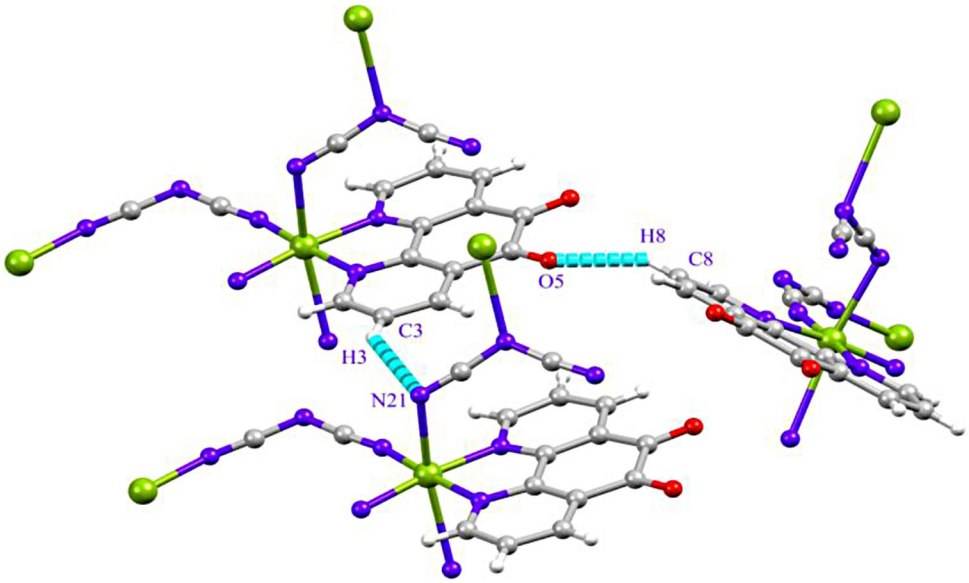

Fig. 4 C-H···N and C-H···O hydrogen bond interactions in compound **1**

Table 4 Short C-N···π and C-O···π contacts (Å, º)

C-X···Cg	X···Cg	C···Cg	C-X···Cg
C24-N25···Cg1^{i}	3.571 (2)	3.171 (2)	87.00 (13)
C24-N25···Cg2^{i}	3.360 (2)	3.496 (2)	87.00 (13)
C24-N25···Cg4^{ii}	2.928 (2)	3.131 (2)	89.03 (14)
C6-O6···Cg4^{iii}	3.118 (2)	4.264 (2)	158.19 (16)

Symmetry codes: (i) *x*, *y*, -1 + *z*; (ii) *x*, *y*, *z*; (iii) x, 1.5-*y*, -0.5 + *z*

Cg1, Cg2 and Cg4 represent the centroids of the rings respectively [Cu(1)-N(1)-C(4B)-C(6B)-N(10), [N(1)-C(2)-C(3)-(4)-C(4 A)-C(4B)], [C(4 A)-C(4B)-C(6B)-C(6 A)-C(6)-C(5), respectively

the crystal packing. The fingerprints of the contacts on the Hirshfeld surface (Fig. 5) were obtained from the software CrystalExplorer17 [47]. The proportion of contacts on the Hirshfeld surface and their enrichment was computed with the MoProViewer software [48]. The contact enrichment ratio E_{xy} between chemical species X and Y is obtained by comparing the actual contacts C_{xy} in the crystal with those computed as if all types of contacts had the same probability to form [49]. Contacts with E_{xy} values larger than unity are

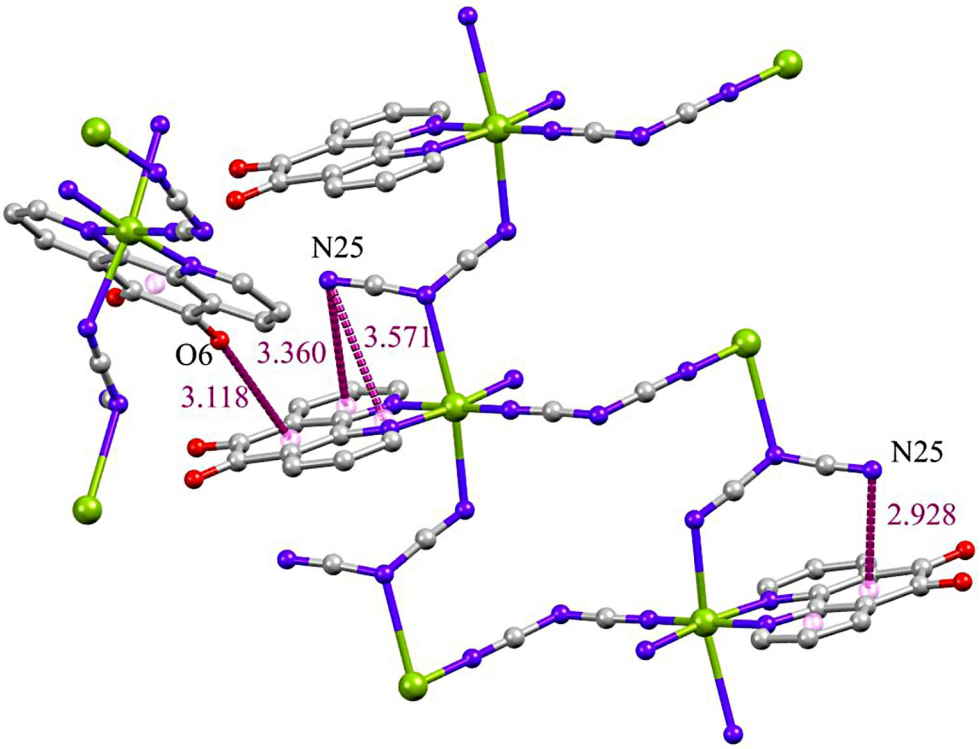

Fig. 5 C-N···π and C-O···π interactions in the structure in compound **1**

Table 5 Analysis of contacts on the Hirshfeld surface. Reciprocal contacts X···Y and Y···X are merged. The second line shows the chemical content on the surface. The surface content, the proportion of contact types between chemical species is given followed by their enrichment ratio. The major contacts as well as the major enriched ones are highlighted in bold characters. In order to obtain integral Hirshfeld surfaces around each of the 4 moieties constituting the asymmetric unit, the calculation was performed on an ensemble of entities in the crystal packing that are not in contact with each other. At the end of the table, the contacts were regrouped in terms of hydrophobic (C and H) and hydrophilic (N, o, Cu^{2+}) atoms

Atom	H	C	*N*	O	Cu
Surface %	18.1	38.9	26.1	7.7	9.2
H	0.8	**16.4**			
C	**12.5**	**14.5**	% contacts		
N	**12.0**	7.5	0.4	0.2	0
O	6.1	4.1	1.4	0.1	
Cu	1.6		**21.6**		
H	0.26	1.30			
C	1.05	0.81	enrichment		
N	**1.42**	1.35	0.06		
O	2.33	0.40	0.37	0.27	0
Cu	0.34		**3.10**	0.06	
	H_{Phob}	H_{Phil}	H_{Phob} x H_{Phil}		
Surface %	57.0	43.0	45.8		
Contacts %	29.7	23.7	0.93		
Enrichment	0.91	1.28			

over-represented. The chemical nature of contacts and their enrichment in the crystal structure are shown in Table 5.

The fingerprint plots (Fig. 6) of the interaction distances around the tricyclic molecule show that the Cu···N coordination is the shortest contact with a central spike at small distances. The two other symmetric spikes at short distance correspond to the C-H···O=C weak hydrogen bonds. The distance fingerprint plot is remarkable for the absence of H···H contact at short distances, the closest contacts being at 3.2 Å, which is much larger than values around 2.2 Å generally observed in crystal packings containing organic molecules, which corresponds to about twice the van der Waals radius of the H atom.

The compounds in the asymmetric unit have several strong H-bond acceptors (C=O and C≡N) but only weak C-H donors. The most abundant contact is constituted by the N···Cu^{2+} coordination and it is also most enriched at E_{NCu} = 3.1 (Table 5). The copper cation is surrounded mostly by six nitrogen atoms and does not interact at all with the oxygen atoms. The other major contacts are C···C, C···N, C···H and N···H due to the abundance of C and N atoms.

The weak hydrogen bond O···H-C is the second most enriched contact at E_{OH} = 2.33 and is quite over-represented

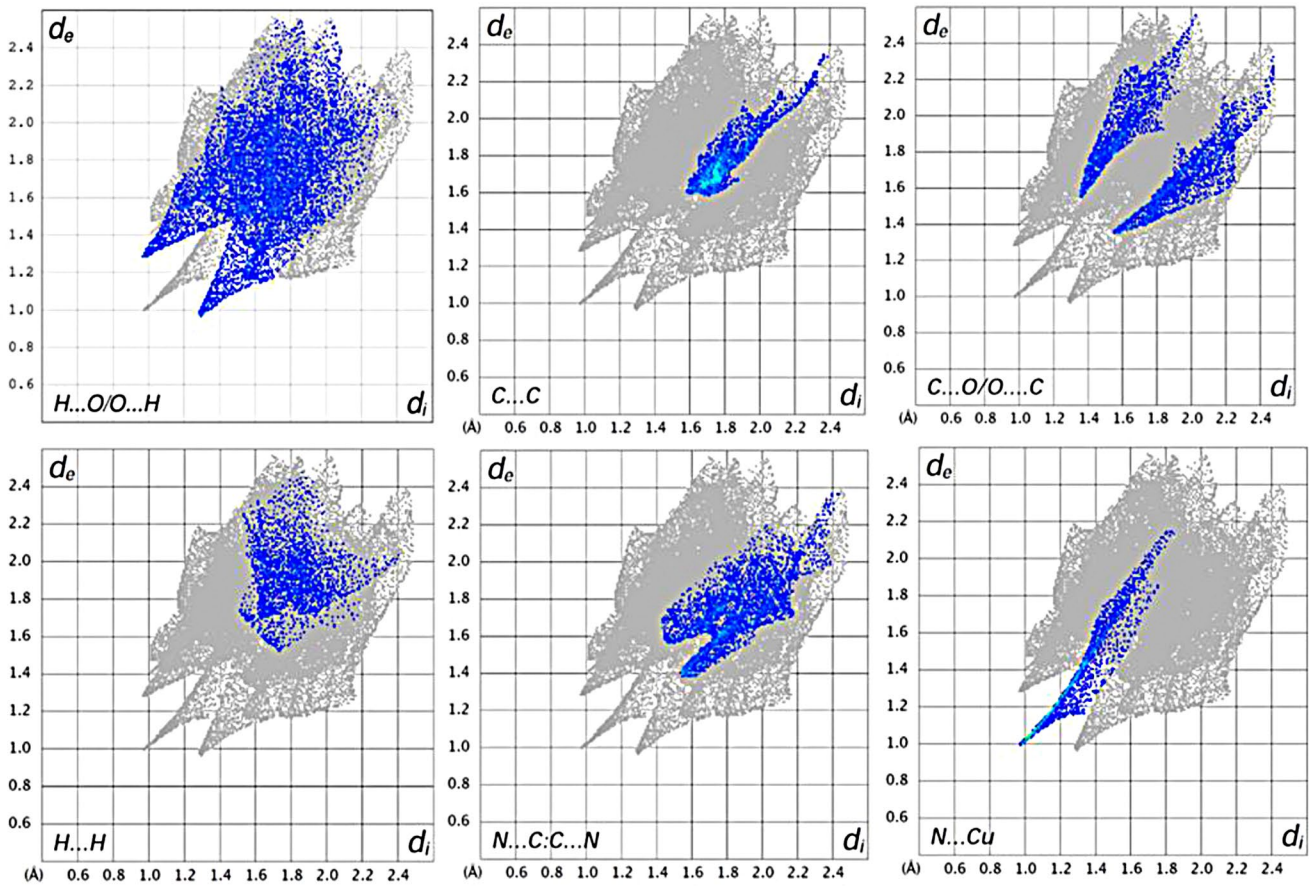

Fig. 6 Fingerprint plots of the main contacts on the Hirshfeld surface around the organic molecule $C_{12}N_2O_2H_6$

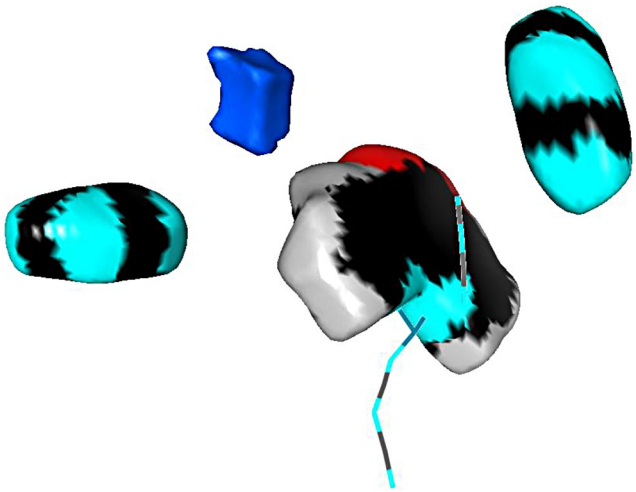

Fig. 7 Hirshfeld surfaces around all moieties constituting the asymmetric unit. The surface is colored according to the inner atom. Carbon: black, hydrogen: grey, oxygen: red, nitrogen: light blue, copper: dark blue

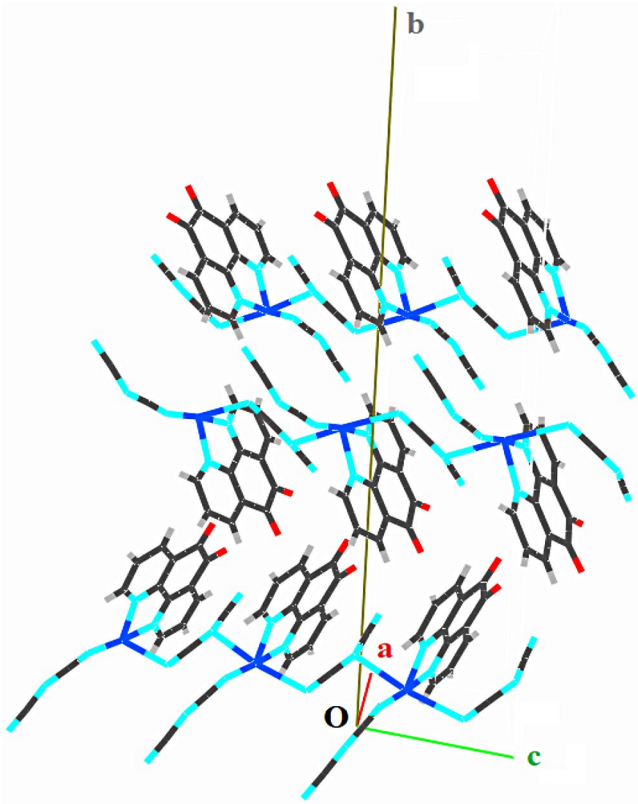

Fig. 8 Autostereogram along the **c** axis. (**a** horizontal, **b** vertical) showing the crystal packing. A short O…C = O bond at 2.931 Å distance is shown as dotted line

at E_{xy}=2.33. The N···H-C hydrogen bonds are more abundant, but less enriched, as the nitrogen atoms are involved in the coordination of the copper cation.

To obtain an integral Hirshfeld surface around each moiety (Cu^{2+} cation and the three organic ligands), a set of entities not in contact with each other in the crystal packing were selected (Fig. 7).

The C···C contacts are quite abundant and are moderately over-represented. Heterocycles have a good propensity to form aromatic stacking due to the possibility of electrostatic complementarity between electronegative and electropositive regions within the cycles [50]. The tricyclic organic molecule has notably electropositive C = O carbon atoms. Moreover, the dicyanamide anion, $NCNCN^-$ bears electronegative carbon atoms that are accessible at the molecular surface. It has to be noticed that C···O contacts are moderately over-represented (E_{CO}=1.35); there is notably an attractive $C^{\delta+}{=}O^{\delta}\cdots C^{\delta+}{=}O^{\delta-}$ relatively short contact between C5 and O6 atoms (autostereogram in Fig. 8 and also Fig. 6). All self-contacts, except C···C, are avoided with E_{xx} values equal to or close to zero, as they represent electrostatic repulsion.

The Hirshfeld surface around the four moieties of the asymmetric unit is constituted by a majority of hydrophobic atoms (C and H-C), which represent 57% in proportion. When the contacts are regrouped in terms of hydrophobic (H_{phob}) and hydrophilic (H_{phil}) atoms, the contacts between H_{phil} atoms are slightly over-represented (E = 1.28, bottom of Table 5), presumably due to the strong enrichment of the N···Cu^{2+} coordination contacts. On the other hand, the contacts between H_{phil} atoms as well as the cross contacts H_{phob} x H_{phil} are both moderately under-represented.

Theoretical Study

In compound **1**, the theoretical study focuses on the unconventional N···π-hole (CN) and CN···π interactions. Figure 9 shows the molecular electrostatic potential (MEP) surface of compound **1** to investigate the most positive and most negative regions of the molecule. The MEP surface of the asymmetric unit of **1** shows that the most negative region (-57 kcal/mol) corresponds to the N-atom of the nitrile group from the dicyanamide ligand, whereas the most positive region is located around the Cu(II) ion (+ 60 kcal/mol), thus indicating that the interaction between the terminal N15 atom of the nitrile group and the Cu(II) ion is favoured from an electrostatic point of view. Interestingly, the MEP is also positive (+ 5.0 kcal/mol) at the C-atom of the cyano group, whereas the MEP value at the N-atom of the dicyanamide ligand is negative (-29 kcal/mol), thus evidencing the formation of N···π-hole (CN) interactions.

The interaction energy of the self-assembled dimer of **1** is relatively large (ΔE_1 = -10.3 kcal/mol) due to a combination of C-H···N hydrogen bonds, N···C≡N, C≡N···π(py) and N···π intermolecular interactions. To evaluate the contribution of N···C≡N interactions, we have computed a theoretical

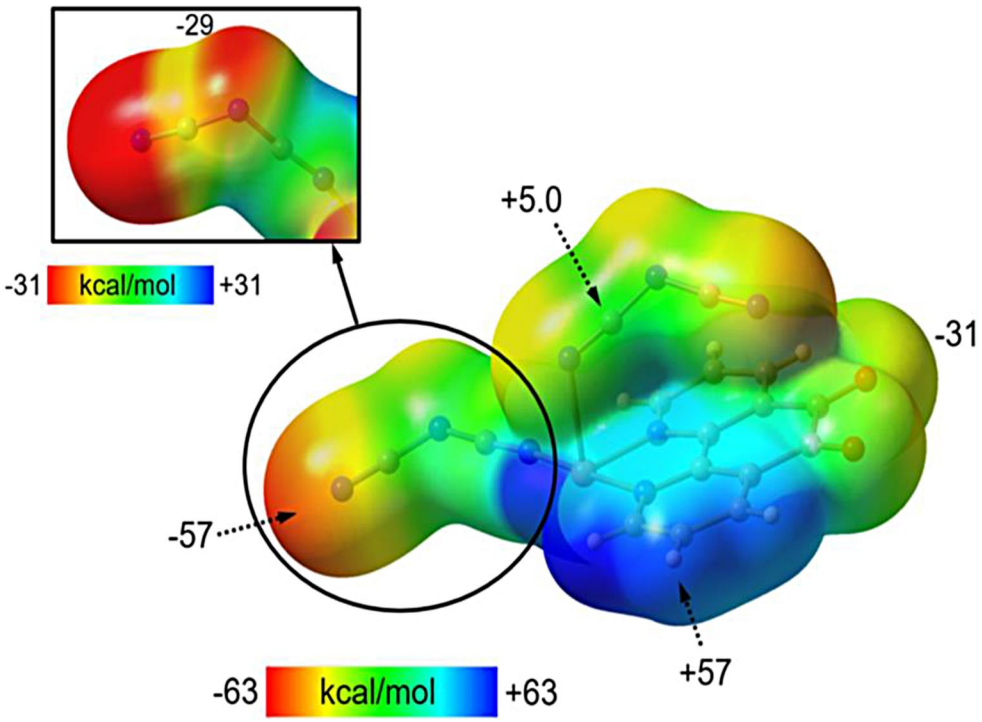

Fig. 9 MEP surface (0.001 a.u. isosurface) of compound **1** computed at M062X/def2-TZVP level of theory

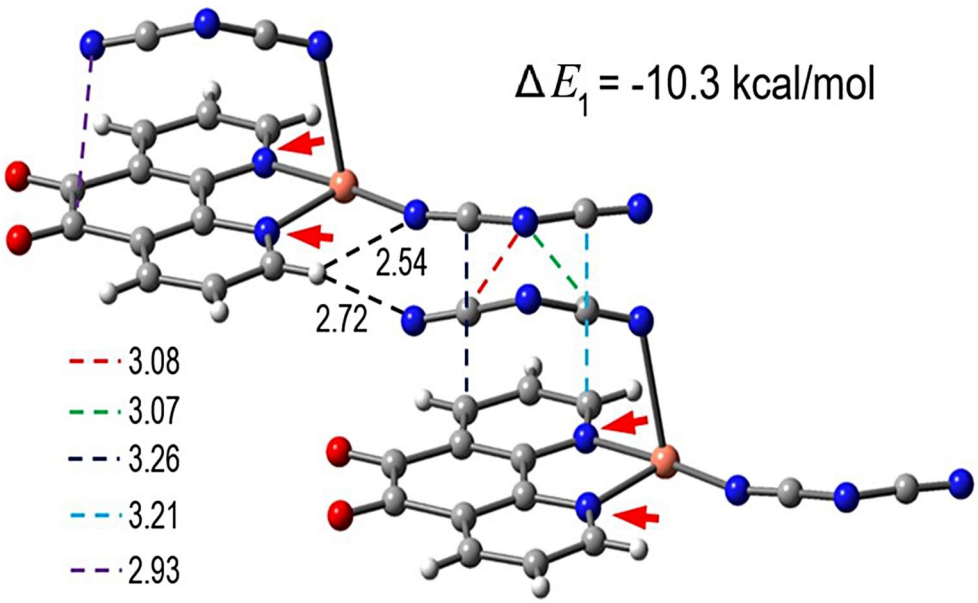

Fig. 10 Self-assembled dimer of **1** showing C-H···N hydrogen bonds (black dashed lines), N···C≡N (red and greed dashed lines), C≡N···π(py) (blue and light blue dashed lines) and N···π (purple dashed lines) interactions. Distances are in Å

model where the pyridine rings coordinated to the Cu(II) atoms were replaced by NH_3 groups (Fig. 10, red arrows). As a result, the interaction energy in this structural model is positive $\Delta E_2 = +3.21$ kcal/mol where the C-H···N hydrogen bonds and C≡N···π(py) and N···π interactions are not formed. This result suggests that the existence of H-bonds, C≡N···π(py) and N···π interactions are necessary for the formation of N···C≡N contacts, indicating a strong cooperativity effect.

Figure 11 shows the distribution of bond CPs and bond paths of the self-assembled dimer mentioned previously. Moreover, the superimposed NCI plot surfaces are also represented. QTAIM analysis of this dimer shows the presence of two bond CPs (small red spheres) and bond paths between the sp^3-hybridized N-atom of the dicyanamide ligand and the C-atoms of the nitrile moiety, thus confirming the formation of N···C≡N interactions. They are characterized by green NCI plot isosurfaces interconnecting the N and C-atoms. Moreover, NBO analysis has also been performed to characterize the N···C≡N interaction. The formation of N···C≡N interaction implies an electron donation from a lone pair of the sp^3 N-atom of the dicyanamide ligand to an empty anti-bonding π* C-N orbital. For the studied compound, the

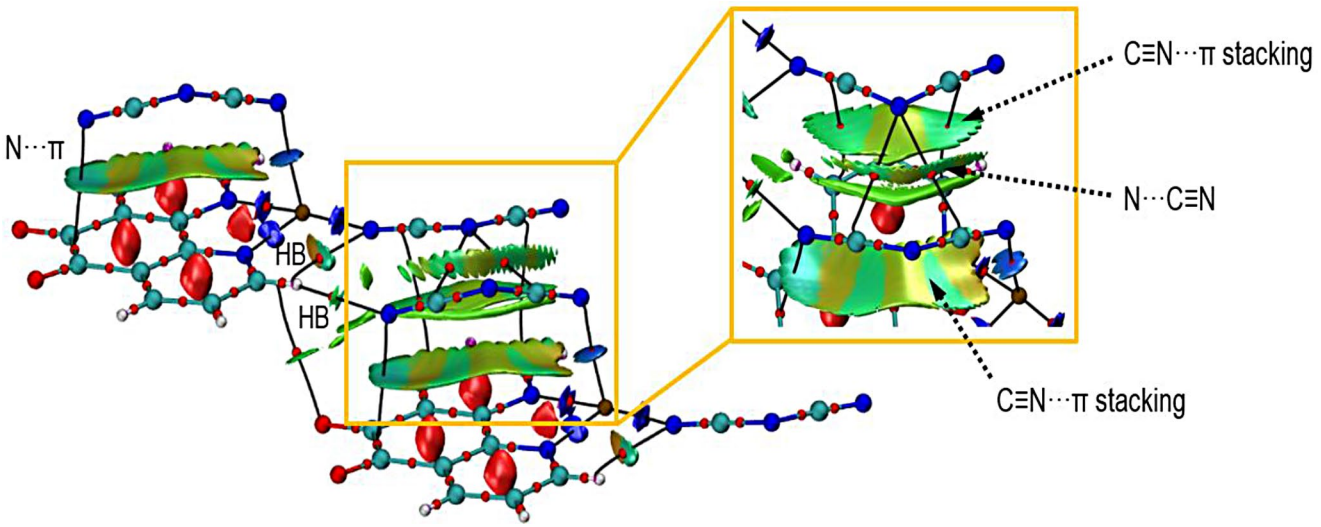

Fig. 11 Combined QTAIM (bond CPs in red and bond paths as black lines) and NCI plot index isosurfaces for a self-assembled dimer of **1**

results revealed the existence of two donor-acceptor orbital interactions, LP N13 → π* C22-N21 and LP N13 → π* C24-N25, with *E*(2) energy values of 0.41 and 0.39 kcal/mol, respectively. It is important to note that the orbital contribution is very low, indicating that the N···C≡N interaction is dominated by electrostatic and dispersion effects, in accordance with the MEP results. Thus, this noncovalent contact can be defined as an N···C≡N (π-hole) interaction.

As shown in Fig. 11, two large NCI plot isosurfaces are located between the nitrile moiety and the pyridine ring, thus revealing the existence of C≡N···π(py) stacking interactions. In order to further evidence the existence of C≡N···π(py) stacking interactions and the importance of orbital effects, NBO analysis of the dimer shown in Fig. 10 has been performed. The results show electron donation from the occupied π (C-C) orbital of the pyridine ring to the antibonding (C-N) orbital of the dicyanamide ligand, with a concomitant stabilization energy of 0.16 kcal/mol. The existence of such electron donations is an indicative of the presence of C≡N···π(py) stacking interactions.

The existence of C-H···N hydrogen bonds is confirmed by QTAIM analysis, which shows for each contact a bond cp. and bond path interconnecting the H and N-atoms. Finally, the presence of N···π interactions has been confirmed by the presence of a bond CP, bond path and green isosurfaces between the terminal N-atom of the nitrile moiety and the C-atom of the carbonyl group in the combined QTAIM/NCI plot analysis.

Concluding Remarks

A new mixed-ligand Cu(II) compound, *catena*-poly[bis(dicyanamido)(1,10-phenanthroline-5,6-dione) copper(II)] (**1**) was synthesized and structurally characterized using single-crystal X-ray diffraction. In this compound, the phendione ligand and dicyanamide anions create an unprecedented ladder-type network, with both 1,5-bridging and 1,3-bridging dca anion. Several non-covalent interactions including C-H···N/O hydrogen bonds, C-O···π and C-N···π stacking interactions play an important role in structural stabilization. The identification of non-covalent interactions was accomplished by the utilization of Hirshfeld surface analysis. Theoretical calculations on the supramolecular trinuclear unit observed in the crystal structure of **1** reveal that also H-bonding interactions combined with the N···π-stacking contacts play an important role in the solid-state stability of compound **1**. The presence of two large NCI isosurfaces located between the nitrile moiety and the pyridine ring, reveals the existence of C≡N···π(py) stacking interactions.

Acknowledgements FS thanks the Algerian MESRS & DGRSDT for financial support (PRFU project B00L01UN190120230003 funds). JE thanks the Spanish MCIN for project PID2022-140244NB-I00 and grant RYC-2017-22853. DMG thanks CONICET (PIP 215), ANPCyT (PICT-serie A-02988) and Secretaria de Ciencia, Arte e Innovacción Tecnológica, SCAIT-UNT (Project 728) for financial support.

Author Contributions 1. The XRD was done jointly by Dr. Hela Ferjani (Data collection) and Prof. Christopher Glidewell (refinement and structure description). 2. The preparation and characterisation was done by Yaakoub Saadalla (PhD student, supervised by Zouaoui Setifi)0. 3. Christian Jelsch performed the Hirshfield surface analysis, 4. Diego M. Gil performed the DFT calculations together with Jorge Echeverria 5. The general supervision came from Fatima Setifi and Zouaoui Setifi.6. General coordination, structure interpretation, writing the first draft and supervision the final draft, as well as journal submission, was done by Jan Reedijk,

Data Availability No datasets were generated or analysed during the current study.

Declarations

Competing Interests The authors declare no competing interests.

References

1. Ribas J, Escuer A, Monfort M, Vicente R, Cortés R, Lezama L, Rojo T (1999) Polynuclear NiII and MnII azido bridging complexes. Structural trends and magnetic behavior. Coord Chem Rev 193:1027–1068. https://doi.org/10.1016.S0010-8545(99)00051-X.
2. Dey SK, Mondal N, El Fallah MS, Vicente R, Escuer A, Solans X, Font-Bardia M, Matsushita T, Gramlich V, Mitra S (2004) Crystal Structure and Magnetic Interactions in Nickel (II) Dibridged complexes formed by two azide groups or by both Phenolate Oxygen – Azide,– Thiocyanate,– carboxylate, or – cyanate groups. Inorg Chem 43(7):2427–2434. https://doi.org/10.1021/ic0352553
3. Barasinski A, Sobczak P, Drzewinski A, Kamieniarz G, Bienko A, Mrozinski J, Gatteschi D (2010) Anisotropy and magnetic properties of the bimetallic thiocyanate-bridged chains: density-matrix renormalization approach. Polyhedron 29(5):1485–1491. https://doi.org/10.1016/j.poly.2010.01.002
4. Malecki JG, Palion J, Oboz M, Gron T (2014) Bimetallic thiocyanate bridged Co(II)-Hg(II) polymers with pyrazole and imidazole ligands. Polyhedron 73:81–86. https://doi.org/10.1016/j.poly.2014.02.015
5. Neumann T, Ceglarska M, Germann LS, Rams M, Dinnebier RE, Suckert S, Jess I,Näther C (2018) Structures, thermodynamic relations, and magnetism of stable and Metastable Ni(NCS) < sub > 2 coordination polymers. Inorg Chem 57(6):3305–3314. https://doi.org/10.1021/acs.inorgchem.8b00092
6. Wang P, Wang YY, Chi YH, Wei W, Zhang SG, Cottrill E, Shi JM (2013) Synthesis, crystal structure, and magnetism of a 1-D cu < SUP > II chain complex with a mono-bromide bridge. J Coord Chem 66(17):3092–3099. https://doi.org/10.1080/00958972.2013.826349
7. Báuza A, Frontera A, Mooibroek TJ (2016) π-Hole interactions involving Nitro compounds: directionality of Nitrate Esters. Cryst Growth Des 16(9):5520–5524. https://doi.org/10.1021/acs.cgd.6b00989
8. Frontera A, Gamez P, Mascal M, Mooibroek TJ, Reedijk J (2011) Putting Anion-π interactions into perspective. Angew Chem -Int Edit 50(41):9564–9583. https://doi.org/10.1002/anie.201100208
9. van Albada GA, Quiroz-Castro ME, Mutikainen I, Turpeinen U, Reedijk J (2000) The first structural evidence of a polymeric cu(II) compound with a bridging dicyanamide anion: X-ray structure, spectroscopy and magnetism of catena-[polybis(2-aminopyrimidine)copper(II)-bis(μ-dicyanamido)]. Inorg Chim Acta 298(2):221–225. https://doi.org/10.1016/s0020-1693(99)00466-1
10. Majumder A, Pilet G, Rodriguez MTG, Mitra S (2006) Synthesis and structural characterisation of three dicyanamide complexes with mn (II), zn (II) and cd (II): supramolecular architectures stabilised by hydrogen bonding. Polyhedron 25(13):2550–2558. https://doi.org/10.1016/j.poly.2006.03.021
11. Mohamadou A, van Albada GA, Kooijman H, Wieczorek B, Spek AL, Reedijk J (2003) The binding mode of the ambidentate ligand dicyanamide to transition metal ions can be tuned by bisimidazoline ligands with H-bonding donor property at the rear side of the ligand. New J Chem 27(6):983–988. https://doi.org/10.1039/b212059c
12. Riggio I, van Albada GA, Ellis DD, Spek AL, Reedijk J (2001) Synthesis, X-ray structure, spectroscopy and magnetism of polymeric bis(μ-dicyanamido)(μ-pyrimidine)copper(II) monoacetonitrile; a 3D compound with bridging dicyanamide anions in two dimensions. Inorg Chim Acta 313(1–2):120–124. https://doi.org/10.1016/s0020-1693(00)00374-1
13. Pal P, Konar S, Lama P, Das K, Bauzá A, Frontera A, Mukhopadhyay S (2016) On the importance of Noncovalent Carbon-Bonding interactions in the stabilization of a 1D co(II) polymeric chain as a precursor of a novel 2D coordination polymer. J Phys Chem B 120(27):6803–6811. https://doi.org/10.1021/acs.jpcb.6b04046
14. Zhang XY, Li B, Zhang JP (2016) An efficient strategy for self-assembly of DNA-Mimic homochiral 1D helical cu(II) chain from Achiral flexible ligand by spontaneous resolution. Inorg Chem 55(7):3378–3383. https://doi.org/10.1021/acs.inorgchem.5b02785
15. Wurzenberger MH, Lechner JT, Stierstorfer J (2020) Copper (II) Dicyanamide Complexes with N-Substituted tetrazole ligands–energetic coordination polymers with moderate sensitivities. ChemPlusChem 85(4):769–775. https://doi.org/10.1002/cplu.202000156
16. Gaspar AB, Munoz MC, Real JA (2004) Clathration effects on the interpenetration in the 2D (4, 4) coordination polymer [[Fe (4, 4′-bipy)$(dca)_2$]·bt]. Inorg Chem Commun 7(6):815–817. https://doi.org/10.1016/j.inoche.2004.05.005
17. Setifi Z, Setifi F, Saadi M, Rouag DA, Glidewell C (2014) *catena*-Poly 4-amino-3,5-bis(pyridin-2-yl)-4*H*-1,2,4-triazole-$\kappa_2 N_1,N_5$ (dicyanamido-κ*N*)copper(II) -μ_2-dicyan-amido-$\kappa_2 N:N$: coordination polymer chains linked into a bilayer by hydrogen bonds and π-π stacking interactions. Acta Crystallogr Sect C-Struct Chem 70:359–. https://doi.org/10.1107/s205322961400504x
18. van Albada GA, Ghazzali M, Al-Farhan K, Reedijk J (2012) A new polymeric Cu(II) compound with double bridging dicyanamide. Synthesis, X-ray structure and spectroscopy of catena-poly-*trans*-bis(4-methyl-pyrimidine-κN1)copper(II)-bis(μ-dicyanamido-κ2-N1,*N5*). Inorganic Chemistry Communications 19:58–60. https://doi.org/10.1016/j.inoche.2012.02.002
19. Van Albada GA, Mutikainen P, Turpeinen U, Reedijk J (2006) A rare 2D structure of a novel Cu(II) dinuclear-based compound with dicyanamide and 4-nitropyridine-N-oxide as ligands. Inorg Chem Commun 9(5):441–443. https://doi.org/10.1016/j.inoche.2006.02.006
20. van Albada GA, van der Horst MG, Mutikainen I, Turpeinen U, Reedijk J (2007) An alternating chain consisting of dinuclear cu(II) ions bridged by bonded end-on bis(μ-dicyanamido-κ*NI,N5*) ligands and hydrogen-bonded pairs of bis(pyrimidin-2-yl)amines, with unusually long Cu•••Cu distances of 7.20 and 9.99 Å:: synthesis, structure and magnetic properties of Cu(dipm)(μ-dca)$(H_2O)(ClO_4)_2$•2EtOH. Inorg Chem Commun 10(9):1014–1018. https://doi.org/10.1016/j.inoche.2007.05.018
21. Kurmoo M, Kepert CJ (1998) Hard magnets based on transition metal complexes with the dicyanamide anion, $[N(CN)_2]$. New J Chem 22(12):1515–1524. https://doi.org/10.1039/A803165G
22. Jensen P, Batten SR, Fallon GD, Hockless DC, Moubaraki B, Murray KS, Robson R (1999) Synthesis, Structural Isomerism,

and Magnetism of Extended Framework compounds of type $[Cu(dca)_2(pyz)]_n$, where dca = dicyanamide ($N(CN)_2$) and pyz = pyrazine. J Solid State Chem 145(2):387–393. https://doi.org/10.1006/jssc.1998.8082
23. Dong W, Wang Q-L, Liu Z-Q, Liao D-Z, Jiang Z-H, Yan S-P, Cheng P (2003) Syntheses, structures and magnetic properties of 1-D complex $[[Ni(\mu1, 5\text{-dca})(pn)_2](ClO_4)]_n$, 2-D complex $[Mn(\mu1, 5\text{-dca})_2(phen)]_n$ and 3-D complex $[Mn(\mu1, 5\text{-dca})_2L]_n$ (dca = dicyanamide, $N(CN)_2^-$; pn = 1, 3-propane diamine; phen = phenanthroline; L = 4, 4′-ditriazole methane). Polyhedron 22(25–26):3315–3319. https://doi.org/10.1016/S0277-5387(03)00476-5
24. Hembury GA, Borovkov VV, Inoue Y (2008) Chirality-sensing supramolecular systems. Chem Rev 108(1):1–73. https://doi.org/10.1021/cr050005k
25. Miller JS (2011) Magnetically ordered molecule-based materials. Chem Soc Rev 40(6):3266–3296. https://doi.org/10.1039/c0cs00166
26. Kahn O (2021) Molecular magnetism, 2nd edn. Courier Dover
27. Maheswari PU, Modec B, Pevec A, Kozlevcar B, Massera C, Gamez P, Reedijk J (2006) Crystallographic evidence of nitrate-π interactions involving the electron-deficient 1,3,5-triazine ring. Inorg Chem 45(17):6637–6645. https://doi.org/10.1021/ic060101j
28. Wang D-X, Wang M-X (2013) Anion – π interactions: generality, binding strength, and structure. J Am Chem Soc 135(2):892–897. https://doi.org/10.1021/ja310834w
29. Thakuria R, Nath NK, Saha BK (2019) The nature and applications of π–π interactions: a perspective. Cryst Growth Des 19(2):523–528. https://doi.org/10.1021/acs.cgd.8b01630
30. Moulton B, Zaworotko MJ (2001) From molecules to crystal engineering: supramolecular isomerism and polymorphism in network solids. Chem Rev 101(6):1629–1658. https://doi.org/10.1021/cr9900432
31. Sheldrick GM (2015) SHELXT–Integrated space-group and crystal-structure determination. Acta Crystallogr Sect A: Found Adv 71(1):3–8. https://doi.org/10.1107/S2053273314026370
32. Sheldrick GM (2015) Crystal structure refinement with SHELXL. Acta Cryst (C) 71:3–8. https://doi.org/10.1107/S2053229614024218
33. Rigaku OD (2015) Crysalis Pro. in *Rigaku Oxford Diffraction Ltd, Yarnton, Oxfordshire, England*
34. Macrae CF, Sovago I, Cottrell SJ, Galek PT, McCabe P, Pidcock E, Platings M, Shields GP, Stevens JS, Towler M (2020) Mercury 4.0: from visualization to analysis, design and prediction. J Appl Crystallogr 53(1):226–235. https://doi.org/10.1107/S1600576719014092
35. Zhao Y, Truhlar DG (2008) The M06 suite of density functionals for main group thermochemistry, thermochemical kinetics, noncovalent interactions, excited states, and transition elements: two new functionals and systematic testing of four M06-class functionals and 12 other functionals. Theor Chem Acc 120:215–241. https://doi.org/10.1007/s00214-007-0310-x
36. Weigend F (2006) Accurate coulomb-fitting basis sets for H to Rn. Phys Chem Chem Phys 8(9):1057–1065. https://doi.org/10.1039/b515623h
37. Frisch M, Trucks G, Schlegel HB, Scuseria G, Robb M, Cheeseman J, Scalmani G, Barone V, Petersson G, Nakatsuji H (2016) Gaussian 16. Gaussian, Inc., Wallingford, CT, USA
38. Boys SF, Bernardi F (1970) The calculation of small molecular interactions by the differences of separate total energies. Some procedures with reduced errors. Mol Phys 19(4):553–566. https://doi.org/10.1080/00269877000101561
39. Bader RF (1991) A quantum theory of molecular structure and its applications. Chem Rev 91(5):893–928. https://doi.org/10.1021/cr00005a013
40. Lu T, Chen F (2012) Multiwfn: a multifunctional wavefunction analyzer. J Comput Chem 33(5):580–592. https://doi.org/0.1002/jcc.22885
41. Humphrey W, Dalke A, Schulten K (1996) VMD: visual molecular dynamics. J Mol Graph 14(1):33–38. https://doi.org/10.1016/026307855(96)00018-5
42. Johnson ER, Keinan S, Mori-Sánchez P, Contreras-García J, Cohen AJ, Yang W (2010) Revealing noncovalent interactions. J Am Chem Soc 132(18):6498–6506. https://doi.org/10.1021/ja100936w
43. Foster J, Weinhold F (1980) Natural hybrid orbitals. J Am Chem Soc 102(24):7211–7218. https://doi.org/10.1021/ja00544a007
44. Groom CR, Bruno IJ, Lightfoot MP, Ward SC (2016) The Cambridge Structural Database. Acta Cryst (B) 72:171–179. https://doi.org/10.1107/S2052520616003954
45. Wu A-Q, Zheng F-K, Cai L-Z, Guo G-C, Mao J-G, Huang J-S (2003) One-dimensional chain structure of catena-poly [[[(1, 10-phenanthroline) copper (II)]-μ-dicyanamido] perchlorate]. Acta Crystallogr Sect E: Struct Rep Online 59(5):m257–m259. https://doi.org/10.1107/S1600536803007438
46. Wood PA, Allen FH, Pidcock E (2009) Hydrogen-bond directionality at the donor H atom—analysis of interaction energies and database statistics. CrystEngComm 11(8):1563–1571. https://doi.org/10.1039/b902330e
47. Spackman PR, Turner MJ, McKinnon JJ, Wolff SK, Grimwood DJ, Jayatilaka D, Spackman MA (2021) CrystalExplorer: a program for Hirshfeld surface analysis, visualization and quantitative analysis of molecular crystals. J Appl Crystallogr 54(3):1006–1011. https://doi.org/10.1107/S1600576721002910
48. Guillot B, Enrique E, Huder L, Jelsch C (2014) MoProViewer: a tool to study proteins from a charge density science perspective. Acta Cryst 70:C279. https://doi.org/10.1107/S2053273314097204
49. Jelsch C, Ejsmont K, Huder L (2014) The enrichment ratio of atomic contacts in crystals, an indicator derived from the Hirshfeld surface analysis. IUCrJ 1:119–128
50. Martinez CR, Iverson BL (2012) Rethinking the term pi-stacking. Chem Sci 3(7):2191–2201. https://doi.org/10.1039/C2SC0045G

Authors and Affiliations

Yaakoub Saadallah[1] · Zouaoui Setifi[1,2] · Hela Ferjani[3] · Christopher Glidewell[4] · Christian Jelsch[5] · Fatima Setifi[1] · Diego M. Gil[6] · Jorge Echeverria[7] · Jan Reedijk[8]

✉ Fatima Setifi
fat_setifi@yahoo.fr

✉ Diego M. Gil
diego.gil@fbqf.unt.edu.ar

✉ Jan Reedijk
reedijk@chem.leidenuniv.nl

Yaakoub Saadallah
saadallahyaakoub292@gmail.com

Zouaoui Setifi
setifi_zouaoui@yahoo.fr

Hela Ferjani
hhferjani@imamu.edu.sa

Christopher Glidewell
cg@st-andrews.ac.uk

Christian Jelsch
christian.jelsch@univ-lorraine.fr

Jorge Echeverria
jorge.echeverria@unizar.es

[1] Laboratoire de Chimie, Ingénierie Moléculaire et Nanostructures (LCIMN), Université, Ferhat Abbas Sétif 1, Sétif 19000, Algeria

[2] Département de Technologie, Faculté de Technologie, Université 20 Août 1955- Skikda, Skikda 21000, Algeria

[3] Center for Innovation and Entrepreneurship, Imam Mohammad Ibn Saud Islamic University (IMSIU), Riyadh 11623, Kingdom of Saudi Arabia

[4] School of Chemistry, University of St Andrews, St Andrews, Fife KY16 9ST, UK

[5] CRM2, CNRS, Université de Lorraine, Nancy 54000, France

[6] Instituto de Química Orgánica, Facultad de Bioquímica, Química y Farmacia, INBIOFAL (CONICET – UNT), Universidad Nacional de Tucumán, Ayacucho 471, San Miguel de Tucumán T4000INI, Argentina

[7] Instituto de Síntesis Química y Catálisis Homogénea (ISQCH) and Departmento de Química Inorgánica, Facultad de Ciencias, Universidad de Zaragoza, Pedro Cerbuna 12, Zaragoza 50009, Spain

[8] Leiden Institute of Chemistry, Leiden University, PO Box. 9502, Leiden, RA 2300, The Netherlands